# ICA APPLIED TO ATRIAL FIBRILLATION ANALYSIS

*José Joaquín Rieta* [1], *Francisco Castells* [1], *César Sánchez* [1] *and Jorge Igual* [2]

[1] Bioengineering, Electronic and Telemedicine Research Group. [2] Department of Communications
Polytechnic University of Valencia, Ctra. Nazaret–Oliva S/N, 46730 Gandía (Valencia), Spain
e–mail: {jjrieta, fracasra }@upv.es

**ABSTRACT**

In this work we present a new biomedical application of independent component analysis (ICA) to solve the problem of atrial activity (AA) extraction from real electrocardiogram (ECG) recordings of atrial fibrillation (AF). The proper analysis and characterization of AA from ECG recordings requires, as a first step, the cancellation of ventricular activity (VA). The present contribution demonstrates the appropriateness of ICA to solve this problem based on three considerations: firstly AA and VA are generated by independent bioelectric sources, secondly AA and VA are subgaussian and supergaussian activities, respectively, and finally the surface ECG can be regarded as an instantaneous linear mixing process. After ICA algorithm application to recordings from 7 patients in AF, we prove that the AA source can be identified using a kurtosis-based reordering of the separated sources and a ulterior spectral analysis for those sources with subgaussian kurtosis.

## 1. INTRODUCTION

Biomedicine is one important research area where ICA techniques has proven their success. The use of ICA in electroencephalography, magnetoencephalography [1], or in the extraction of the fetal electrocardiogram (ECG) from maternal recordings [2] are some examples of it. In the ECG, ICA also has been applied to the separation of breathing artifacts, and other disturbances [3]. The present work shows a new application of ICA for the extraction of AA from the ECG in atrial fibrillation (AF) episodes. AF is the most common sustained arrhythmia encountered by clinicians and occurs in approximately 0,4% to 1,0% of the general population. Its prevalence increases with age, and up to 10% of the population older than 80 years has been diagnosed with AF [4].

The proper analysis and characterization of AF from ECG recordings –regardless of the leads considered– requires the extraction or cancellation of the signal components associated to ventricular activity (VA), that is, the QRS complex and the T wave (QRS–T). Unfortunately, a number of facts hinder this operation: AA presents much lower amplitude than VA, and both possess spectral contents notably overlapped, rendering linear filtering solutions unsuccessful.

Methods reported in the literature to cancel VA in the ECG involve direct suppression of the QRS–T complex through the subtraction of a mean QRS–T template [5, 6]. Also the correct spatiotemporal alignment of every complex before cancellation has proven to be very effective [7]. More recent methods have focused on extracting the VA using artificial neural networks [8], or decomposing the ECG in a set of coefficients obtaining the AA via discrete packet wavelet transform [9]. Nevertheless, one common limitation of all the previously mentioned methods is their inability to obtain a unified AA signal from a multi–lead ECG.

The observation that AA and VA are decoupled [6] introduces a new separation perspective which does not rely on direct QRS–T elimination. We can assume that AA and VA are generated by physically –and hence statistically– independent sources of bioelectric current [4, 7]. Hence, atrial and ventricular source contributions appear mixed in the ECG and can be separated via a suitable blind signal separation (BSS) method.

Two BSS techniques has been proposed based on principal component analysis (PCA) [10, 11] and independent component analysis (ICA) [12]. PCA–based methods search for a solution that decorrelates the input signals, thus providing optimal results when the independent sources present Gaussian behavior. But the observation that AA and VA do not present random Gaussian distributions [6, 7] makes necessary to impose higher order statistical conditions to separate AA from VA, like ICA–based methods do.

The present contribution proves the appropriateness of ICA to solve the AA extraction problem in real AF episodes, by exploiting the fact that AA and VA are independent sources and that the ECG recordings fulfill the instantaneous linear mixtures model.

## 2. ATRIAL FIBRILLATION DESCRIPTION

One normal cardiac cycle is started at the sinus node with an electrical activation (depolarization) of the right atrium, and spreads towards the entire atria in a well-ordered way. Atrial depolarization defines the P wave of the ECG. Next, depolarization impulse reaches the ventricles and their fast contraction produces the QRS complex of the ECG. Finally, ventricular repolarization produce the T wave and finish the cardiac cycle [13].

Atrial Fibrillation is a supraventricular arrhythmia characterized by uncoordinated atrial activation. AF occurs when the electrical impulses in the atria degenerate from their usual organized pattern into a rapid chaotic pattern [4]. On the ECG, AF is described by the replacement of consistent P waves by rapid oscillations or fibrillatory waves that vary in size, shape, and timing, associated with an irregular, frequently rapid ventricular response.

## 3. ICA APPROACH TO ATRIAL FIBRILLATION

The relevance of ICA in the extraction of AF lies in the fulfillment of three basic considerations: independence of the sources, nongaussianity and observations generated by means of an instantaneous linear mixing model [14]. This scenario will be described in the next sections.

### 3.1. Independence and Nongaussianity

Considering the chaotic and disorganized nature of AA during an AF episode, along with the fact that AA and VA are physically decoupled [4, 7], makes possible to consider both activities as generated by independent bioelectric sources, thus fulfilling the independence requirement for ICA separation. With respect to nongaussianity VA presents high values within the heart beat (QRS complex) and low values in the rest of the cardiac cycle, hence the histogram analysis of VA reveals a supergaussian behavior [6]. On the other hand, AA of an AF episode behaves, statistically speaking, as a subgaussian variable and has been modeled as a saw–tooth signal consisting of a sinusoid with several harmonics [6, 7].

### 3.2. The Forward Problem Formulation

There are several physical models to represent both the cardiac current sources and the enclosing torso shape and conductivity [13]. The combination of torso and source models to calculate the body surface potentials is known as the forward problem [15]. One accepted solution for the forward problem relays on the calculation, using surface methods, of the outer body surface potentials from the epicardial (external surface of the heart) surface potentials [16]. Surface methods are based on integral equations for the potential derived by applying Green's second identity in a torso model comprising two surfaces, the body surface $S_B$ and the heart surface $S_H$. For solving the problem it is assumed that the region contained between the two surfaces is homogenous. In that case, the body surface potential can be expressed as [15, 17]

$$\mathbf{P}_{BB}\mathbf{\Phi}_B + \mathbf{P}_{BH}\mathbf{\Phi}_H + \mathbf{G}_{BH}\mathbf{\Gamma}_H = 0 \tag{1}$$

$$\mathbf{P}_{HB}\mathbf{\Phi}_B + \mathbf{P}_{HH}\mathbf{\Phi}_H + \mathbf{G}_{HH}\mathbf{\Gamma}_H = 0 \tag{2}$$

where $\mathbf{\Phi}_B$ and $\mathbf{\Phi}_H$ are ($1\times N_B$ and $1\times N_H$) column vectors of potentials, $\mathbf{\Gamma}_H$ is a column matrix ($1\times N_H$) of epicardial potential gradients, and the various $\mathbf{P}$ and $\mathbf{G}$ coefficient matrices are determined solely by integrations involving the geometry of the epicardial and body surfaces. The first subscript of $\mathbf{P}$ (or $\mathbf{G}$) represents the surface containing the observation points, having as much rows as points ($N_H$ or $N_B$), and the second one, the surface (heart or body) of integration with the number of columns equal to the number of points where the integration is computed ($N_H$ or $N_B$). By solving equation (2) for the matrix of epicardial potential gradients $\mathbf{\Gamma}_H$ and substituting the result into equation (1) yields

$$\mathbf{\Phi}_B = \mathbf{T}_{BH}\mathbf{\Phi}_H \tag{3}$$

with $\mathbf{T}_{BH}$ defined as

$$\begin{aligned}\mathbf{T}_{BH} = &\left(\mathbf{P}_{BB} - \mathbf{G}_{BH}(\mathbf{G}_{HH})^{-1}\mathbf{P}_{HB}\right)^{-1} \cdot \\ &\cdot\left(\mathbf{G}_{BH}(\mathbf{G}_{HH})^{-1}\mathbf{P}_{HH} - \mathbf{P}_{BH}\right)\end{aligned} \tag{4}$$

Equations (3) and (4) define the solution to the forward problem. The elements of matrix $\mathbf{T}_{BH}$ are the *transfer coefficients* relating the potential at a particular point on the epicardial surface to that at a particular point on the body surface, and they depend solely of the geometry of the epicardial and body surfaces.

### 3.3. ECG Instantaneous Linear Mixture Model

From equation (3) it has been shown the possibility of obtaining the electric potential in one point of the body surface by adding the partial contributions of the heart potentials, each one multiplied by a transfer coefficient. Obviously, equation (3) holds a linear mixing model where a set of *observations* are obtained by linearly combining a set of *sources*.

Moreover, in the description of the volume conductor constituted by the human body, the capacitive component of tissue impedance is negligible in the frequency band of

internal bioelectric events (0–100Hz). Hence, the volume conductor currents generated by the heart require only specification of the tissue resistivity [13]. These considerations imply that time–varying bioelectric currents and voltages in the human body can be examined with the conventional static approximation. That is, all currents and fields behave, at any instant, as if they were stationary and we can assume the fulfillment of the ICA instantaneous linear mixture model for eq. (3).

Since lots of cardiac cells are activated simultaneously, the joint activity of the cardiac cells can be observed by placing at specific locations of the body surface several bioelectric sensors. The signals obtained by these sensors are the multi–lead ECG. The 12–lead ECG comprises the Einthoven *limb leads* (standard leads) with voltages defined as

$$\mathrm{I} = \Phi_L - \Phi_R; \quad \mathrm{II} = \Phi_F - \Phi_R; \quad \mathrm{III} = \Phi_F - \Phi_L \tag{5}$$

where $\Phi_L$ is the potential at the left arm, $\Phi_R$ at the right arm and $\Phi_F$ at the left foot. Other three additional *limb leads* are those defined by Goldberger by measuring the potential between a single limb electrode and the midpotential of the two remaining electrodes, chosen as reference. These additional leads are called augmented leads due to the augmentation of the signal and are defined as

$$\begin{aligned} \mathrm{aVR} &= \Phi_R - \tfrac{1}{2}(\Phi_L + \Phi_F) \\ \mathrm{aVL} &= \Phi_L - \tfrac{1}{2}(\Phi_R + \Phi_F) \\ \mathrm{aVF} &= \Phi_F - \tfrac{1}{2}(\Phi_R + \Phi_L) \end{aligned} \tag{6}$$

Finally, the six precordial leads are located over the left chest, near the heart, and measure the unipolar potential between one point in the thorax and Wilson's Central Terminal (midpoint between the three standard leads) and are defined as

$$\mathrm{V}_i = \Phi_i - \tfrac{1}{3}(\Phi_R + \Phi_L + \Phi_F) \quad i = 1 \cdots 6 \tag{7}$$

where $\Phi_i$ is the surface potential of precordial lead $i$.

The mathematical operations performed in equations (5) to (7) defining the voltages for the 12–lead ECG as a function of the body surface potentials, clearly, do not affect at all to the aforementioned ICA instantaneous linear mixture model, and then, the application of ICA–based methods is completely justified.

Therefore, the three most important considerations in order to apply ICA: instantaneous linear mixtures, independent sources and nongaussianity (thus making unsuitable PCA–based separation techniques), are accomplished for the 12–lead ECG recordings of a patient in AF.

### 3.4. AF Extraction via ICA

If we define the generative ICA model as [1]:

$$\mathbf{x} = \mathbf{A} \cdot \mathbf{s} \tag{8}$$

where $\mathbf{s}$ is the sources vector, $\mathbf{x}$ the observations and $\mathbf{A}$ the mixing matrix, hence, the skin-electrode signal vector of the ECG can be identified with $\mathbf{x}$ and complies with the ICA model, where vector $\mathbf{s}$ is composed of the independent sources of atrial and ventricular cardiac activity and other nuisance signals.

The mixing matrix entries depend on the body geometry, tissue conductivity, electrode position, etc., similarly as occurs in the ICA formulation of the fetal ECG extraction problem [2]. Consequently, the atrial contribution to the recordings can be recovered by extracting, via ICA, the sources of AA and the corresponding columns of the mixing matrix.

All signals were sampled (or re-sampled, if required) at 1 kHz. The signals were preprocessed using a notch filter to cancel out mains interference, and a band–pass filter with cut–off frequencies of 0,5 and 60 Hz to remove baseline wandering and thermal noise [5]. The signal database was comprised of recordings from 7 patients in AF, all of them 12–lead and 8 seconds length.

In this work we have mainly used the FastICA algorithm [18] due to its performance and the ability to estimate every independent component one by one, so the algorithm can be stopped, decreasing computational load, once the AA has been extracted.

The subgaussian model of AA in front of the supergaussian behavior of VA allows the identification of AA using a kurtosis–based reordering. This process will place in one side the subgaussian sources, associated to AA, in the middle the Gaussian ones, associated to noise and other artifacts, and in the other side the supergaussian sources corresponding to VA. Therefore, that separated source with lowest kurtosis will be the AA source.

After reordering, in order to carry out a more AA robust identification, the power spectral density (PSD) was computed for all the separated sources with subgaussian kurtosis ($k < 0$). The procedure consisted of obtaining the modified periodogram from the separated sources using the Welch-WOSA method with a Hamming window of 4096 points length, a 50% overlapping between adjacent windowed sections and a 8192 points length FFT. Later, the spectral content above 20Hz has been discarded due its low contribution. This way, it is possible to observe and compare the spectral content of the separated sources with the accepted spectral content of AF [5, 10, 19, 20, 21].

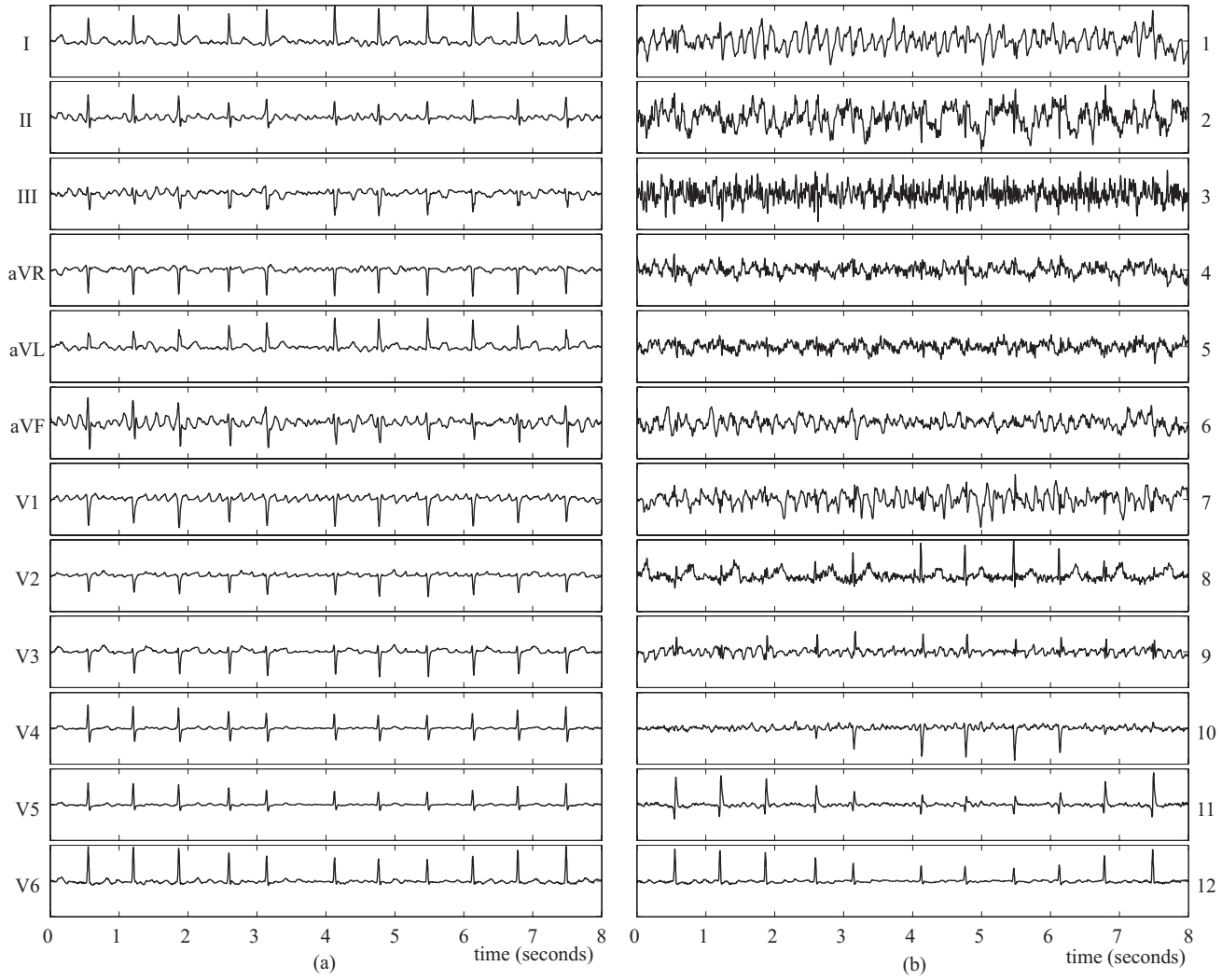


**Fig. 1.** (a) 12–lead ECG from a patient in AF. (b) ICA estimated sources from lower to higher kurtosis. Atrial activity is source #1.

## 4. RESULTS AND DISCUSSION

To perform the AA extraction several ICA algorithms were applied [18, 22] obtaining similar results. Apart from the ICA approach employed, it was always possible to identify the AA source among the whole set of separated sources for all the AF episodes analyzed. The AA identification process was carried out following the aforementioned steps: reordering the sources from lower to higher kurtosis and obtaining the PSD of the sources with $k < 0$. Fig. 1(a) plots a 12–Lead ECG with an AF episode. Observe the fibrillatory waves that can be clearly identified in several leads. Usually is accepted by the scientific community that leads II, III, aVF and V1 have the largest AA content, as can be seen in the Figure.

The result of applying ICA to this AF episode and reordering the estimated sources as a function of its kurtosis generates the sources plot of Fig. 1(b), where source #1 has the lowest kurtosis ($-0{,}7368$) and source #12 has the largest one ($+33{,}045$). Due to the kurtosis reordering, the first separated sources (#1–2) will have a more subgaussian PDF and hence are the candidates to contain the AA, the central sources are associated to Gaussian noise and signal artifacts (#3–7) and, the last sources (#8–12) contain mainly the ventricular activity.

Additionally, a spectral analysis was applied over the sources with subgaussian kurtosis ($k < 0$) to determine the AA source. Fig. 2 plots the results of the PSD calculations for all the negative kurtosis sources. As it can be seen, source #1 presents a typical spectral morphology of the AA from a patient with AF. The pattern of these kind of episodes is characterized by a very pronounced peak in frequencies from 5 to 8Hz, without harmonics and with insignificant amplitudes above 15Hz. In the case of source #1 the main peak frequency is $f_p = 6{,}34$Hz.

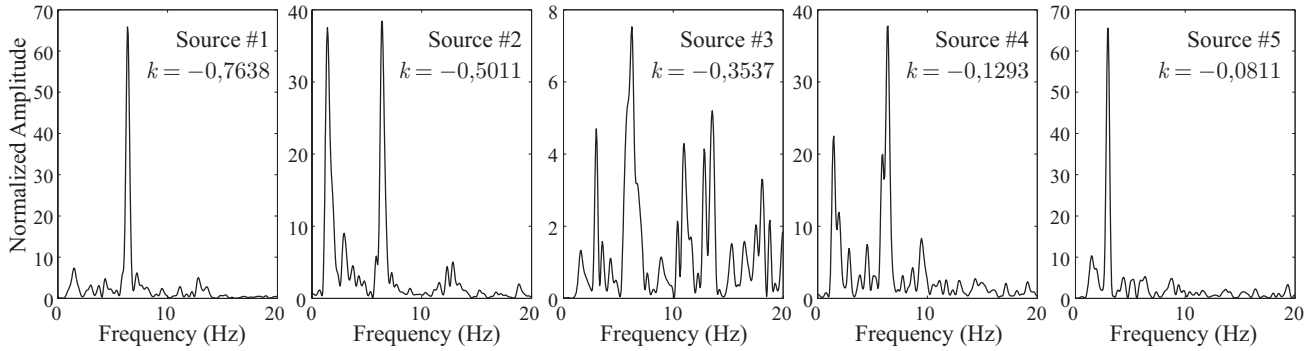


**Fig. 2.** Power spectral densities from several ICA-estimated sources of Fig. 1. After kurtosis-based reordering only five sources have subgaussian kurtosis, and the one with lowest kurtosis (source #1) presents a PSD typically associated with the AA in AF episodes.

Also, it can be seen in Fig. 2 that the only separated source with similar spectral content is source #5, but in this case the main peak frequency is $f_p = 2{,}93$Hz, hence, it have not to be considered as a source with AA content. Moreover, this decision can be reinforced if we take in account its kurtosis ($k_{\#5} = -0{,}081$) near Gaussianity.

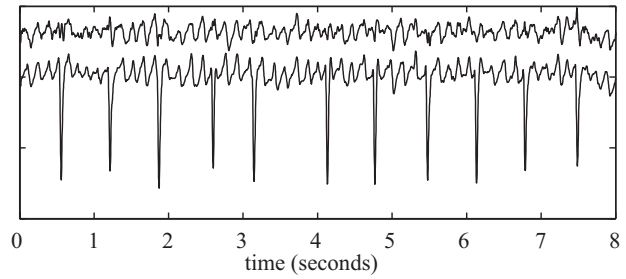


**Fig. 3.** In the upper side, separated source #1 of Fig. 1, associated to AA, multiplied by the scaling factor –0,0675 corresponding to its projection into lead V1. In the lower side, lead V1 of the 12–lead ECG in Fig. 1.

The AA estimate obtained from an ECG in AF via ICA are considered by cardiologists as very approximate to the real atrial waveforms contained in the episode. This outcome is illustrated in Fig. 3 which shows (in the top) the atrial source #1 of Fig. 1 estimated via ICA scaled by the factor $-0{,}0675$ associated to the projection of the estimated AA into lead V1. This lead is usually accepted as the one with the largest AA content and is shown in the bottom of Fig. 3 for visual comparison.

Table 1 shows the projection coefficients of the AA source (#1 in Fig. 1 and 2) to each lead. It can be seen that V1 has the largest contribution. This fact serves as a reinforcement of the separation performance, meaning that the estimated AA has a very close correspondence with the real one contained in the AF episode.

Despite the large visual similarity between the fibrillatory waves of the estimated AA source and the AA contained in lead V1 (see Fig. 3), it must be said that this kind of direct visual comparison, strictly speaking, only has to be considered in a illustrative way, because the obtained AA source via ICA combine AA information from all the ECG leads and not only from V1.

**Table 1**. Coefficients from the column of **A** showing the projection of the AA to each lead in the ECG.

| Lead | Coefficient | Lead | Coefficient |
|---|---|---|---|
| I | 0,0130 | V1 | – 0,0675 |
| II | 0,0217 | V2 | – 0,0157 |
| III | – 0,0278 | V3 | – 0,0123 |
| aVR | – 0,0146 | V4 | 0,0186 |
| aVL | 0,0178 | V5 | – 0,0042 |
| aVF | – 0,0281 | V6 | 0,0081 |

Nevertheless, the only way to corroborate if the AA source separation has been satisfactory, is to compare it with those ECG leads containing the largest atrial activity. This is a typical consequence of the BSS–based methods where the real sources are latent variables that can not be directly observed.

## 5. CONCLUSIONS

The present contribution has shown a new biomedical engineering application for the ICA–based separation methods due to the key observation of three facts: firstly, in atrial arrhythmia episodes the bioelectric sources of the heart generating AA and VA can be regarded as statistically independent. Secondly, both activities present a non–Gaussian behavior and, finally, AA and VA are manifested at the body surface as an instantaneous linear mixture in which the mixture depends on the electrode position of the ECG. These considerations make feasible the application of ICA and this contribution has proven its usefulness to solve the AA extraction problem.

Traditional techniques based on direct cancellation of the QRS–T complex, obtain as much AA signals as leads

has been introduced to the cancellation algorithm. In contrast to this, the ICA–based method is able to obtain one AA signal that considers the contribution present in every lead from the ECG to reconstruct the complete cardioelectric AA. Moreover, as a direct consequence of the method, it is also obtained a new alternative way to QRS–T cancellation in atrial arrhythmia analysis.

After applying ICA to the ECG, the direct visual identification of the AA source is not always possible. Nevertheless, due to the dissimilar statistical properties of AA in contrast to VA, the kurtosis–based reordering of the sources has proven its ability to identify the AA source as the one with lowest kurtosis. In a second step this identification has been validated via spectral analysis of the subgaussian separated sources. The combination of the aforementioned steps constitutes a robust AA identification method.

Finally, these positive results allow the birth of new noninvasive techniques for AF analysis, an hence, are the first step in the future improvement and development of new diagnostic techniques and pathologies prediction.

## ACKNOWLEDGEMENTS

Authors would like to thank Xosé Millet for his valuables scientific contributions and cardiologists Ricardo Ruiz, Salvador Morell and Roberto García Civera for their clinical advises. This work was partially funded by UPV program “Grupos interdisciplinares”.

## REFERENCES

[1] A. Hyvarinen, J. Karhunen, and E. Oja, *Independent Component Analysis* John Wiley & Sons, Inc., 2001.

[2] V. Zarzoso and A. K. Nandi, "Noninvasive fetal electrocardiogram extraction: blind separation versus adaptive noise cancellation", *IEEE Transactions on Biomedical Engineering*, vol. 48, no. 1, pp. 12-18, Jan.2001.

[3] A. K. Barros, A. Mansour, and N. Ohnishi, "Adaptive Blind Elimination of Artifacts in ECG Signals", *International Workshop on Independence & Artificial Neural Networks (I&ANN'98)*, pp. 1380-1386, Feb.1998.

[4] V. Fuster, L. E. Ryden *et al*., “ACC/AHA/ESC guidelines for the management of patients with atrial fibrillation”, *Journal of the American College of Cardiology*, vol. 38, no. 4, pp. 1266-1336, Oct.2001.

[5] A. Bollmann, N. K. Kanuru, K. K. McTeague, P. F. Walter, D. B. DeLurgio, and J. J. Langberg, "Frequency Analysis of Human Atrial Fibrillation Using the Surface Electrocardiogram and Its Response to Ibutilide", *American Journal of Cardiology*, vol. 81, no. 12, pp. 1439-1445, June. 1998.

[6] S. Shkurovich, A. V. Sahakian, and S. Swiryn, "Detection of atrial activity from high-voltage leads of implantable ventricular defibrillators using a cancellation technique", *IEEE Transactions on Biomedical Engineering*, vol. 45, no. 2, pp. 229-234, 1998.

[7] M. Stridh and L. Sornmo, “Spatiotemporal QRST cancellation techniques for analysis of atrial fibrillation”, *IEEE Transactions on Biomedical Engineering*, vol. 48, no. 1, pp. 105-111, Jan.2001.

[8] C. Vasquez, A. Hernandez, F. Mora, G. Carrault, and G. Passariello, "Atrial activity enhancement by Wiener filtering using an artificial neural network", *IEEE Transactions on Biomedical Engineering*, vol. 48, no. 8, pp. 940-944, Aug.2001.

[9] C. Sanchez, J. Millet, J. J. Rieta, J. Rodenas, F. Castells, R. Ruiz, and V. Ruiz, "Packet Wavelet Decomposition: An Approach For Atrial Activity Extraction", *IEEE Computers in Cardiology*, vol. 29 in press Sept.2002.

[10] P. Langley, J. P. Bourke, and A. Murray, "Frequency analysis of atrial fibrillation", *IEEE Computers in Cardiology* , vol. 27 pp. 65-68, 2000.

[11] L. Faes, G. Nollo, M. Kirchner, E. Olivetti, F. Gaita, R. Riccardi, and R. Antolini, "Principal component analysis and cluster analysis for measuring the local organisation of human atrial fibrillation", *Medical & Biological Engineering & Computing*, vol. 39, no. 6, pp. 656-663, Nov.2001.

[12] J. J. Rieta, V. Zarzoso, J. Millet, R. Garcia, and R. Ruiz, “Atrial Activity Extraction Based on Blind Source Separation as an Alternative to QRST Cancellation for Atrial Fibrillation Analysis”, *IEEE Computers in Cardiology*, vol. 27 pp. 69-72, Sep. 2000.

[13] J. Malmivuo and R. Plonsey, *Bioelectromagnetism: Principles and Applications of Bioelectric and Biomagnetic Fields*, Oxford University Press, 1995.

[14] J. F. Cardoso, "Blind signal separation: Statistical principles", *Proceedings of the IEEE*, vol. 86, no. 10, pp. 2009-2025, Oct.1998.

[15] R. M. Gulrajani, "The forward and inverse problems of electrocardiography", *IEEE Engineering in Medicine and Biology Magazine*, vol. 17, no. 5, pp. 84-101, 1998.

[16] R. C. Barr, T. C. Pilkington, J. P. Boineau, and M. S. Spach, "Determining surface potentials from current dipoles, with application to electrocardiography", *IEEE Transactions on Biomedical Engineering*, vol. 13 pp. 88-92, Apr.1966.

[17] R. C. Barr, M. Ramsey, and M. S. Spach, "Relating epicardial to body surface potential distribution by means of transfer coefficients based on geometry measurements", *IEEE Transactions on Biomedical Engineering*, vol. 24 pp. 1-11, 1977.

[18] Hurri, J., Gavert, J., Sarela, J., and Hyvarinen, A. The FastICA package for Matlab. 1998. `http://www.cis.hut.fi/projects/ica/fastica`

[19] M. Stridh, L. Sornmo, C. J. Meurling, and S. B. Olsson, "Characterization of atrial fibrillation using the surface ECG: time-dependent spectral properties", *IEEE Transactions on Biomedical Engineering*, vol. 48, no. 1, pp. 19-27, Jan.2001.

[20] J. J. Rieta, J. Millet, V. Zarzoso, F. Castells, C. Sanchez, R. Garcia, S. Morell, "Atrial Fibrillation, Atrial Flutter And Normal Sinus Rhythm Discrimination By Means Of Blind Source Separation And Spectral Parameters Extraction", *IEEE Computers in Cardiology*, vol.29 in press 2002.

[21] P. Langley, M. Stridh, J. J. Rieta, L. Sornmo, J. Millet, and A. Murray, "Comparison Of Atrial Rhythm Extraction Techniques For The Detection Of The Main Atrial Frequency From The 12-Lead ECG In Atrial Fibrillation", *IEEE Computers in Cardiology*, vol. 29 in press Sept.2002.

[22] A. Cichocki, S. Amari, K. Siwek et al, ICALAB Toolboxes, 2002. `http://www.bsp.brain.riken.go.jp/ICALAB`